Acta Crystallographica Section F
Structural Biology and Crystallization Communications
ISSN 1744-3091

Cloning, purification and crystallization of MotB, a stator component of the proton-driven bacterial flagellar motor

Jenna O'Neill and Anna Roujeinikova*

Manchester Interdisciplinary Biocentre, Faculty of Life Sciences, University of Manchester, 131 Princess Street, Manchester M1 7DN, England

Correspondence e-mail: anna.roujeinikova@manchester.ac.uk

Received 5 April 2008
Accepted 27 April 2008

MotB is an essential component of the proton motive force-driven bacterial flagellar motor. It binds to the stress-bearing layer of peptidoglycan in the periplasm, anchoring the MotA/MotB stator unit to the cell wall. Proton flow through the channel formed by the transmembrane helices of MotA and MotB generates the turning force (torque) applied to the rotor. Crystals of recombinant *Helicobacter pylori* MotB have been obtained by the sitting-drop vapour-diffusion method using ammonium sulfate as a precipitant. These crystals belong to space group $P4_12_12$ or its enantiomorph $P4_32_12$, with unit-cell parameters a = 75.2, b = 75.2, c = 124.7 Å. The asymmetric unit appears to contain one subunit, corresponding to a packing density of 3.4 Å^3 Da^{-1}. The crystals diffract X-rays to at least 1.8 Å resolution on a synchrotron-radiation source.

1. Introduction

Many bacteria swim through fluids by rotating their helical flagella using membrane-embedded molecular rotary motors (DeRosier, 1998; Blair, 2003). Rotation of the bacterial flagellar motor is powered by the proton motive force (pmf) or, in the case of alkalophiles and marine *Vibrio* species, sodium motive force (Manson *et al.*, 1977; Hirota & Imae, 1983). In pmf-driven motors, the proton flow through the stator ring formed by the proteins MotA and MotB generates the turning force (torque) applied to the rotor *via* an as yet unknown molecular mechanism. The proton channel is formed by the transmembrane (TM) helices of MotA and MotB (Zhou *et al.*, 1998; Blair, 2003). MotB has a short N-terminal cytoplasmic segment, a single TM α-helix and a large periplasmic domain which shares homology with outer membrane protein A-like domains and is therefore believed to bind to the highly cross-linked stress-bearing layer of peptidoglycan of the cell wall (Chun & Parkinson, 1988; DeMot & Vanderleydon, 1994).

Motility by flagellar motor is essential for the virulence of many pathogenic bacteria, including *Helicobacter pylori*, a Gram-negative bacterium that colonizes the stomachs of roughly 50% of the world's population (Covacci *et al.*, 1999). *H. pylori* has a tuft of 4–6 flagella at one end of the cell body that help it drill into the mucus layer of the stomach (Yoshiyama & Nakazawa, 2000). Motility is required during initial colonization (Eaton *et al.*, 1992) and to attain full infection levels (Ottemann & Lowenthal, 2002). *H. pylori* infection has been linked to gastric inflammation and peptic ulcers and is a risk factor for gastric cancer (Uemura *et al.*, 2001). *H. pylori* possesses a single *motB* gene (Tomb *et al.*, 1997), in-frame deletion of which creates flagellated nonmotile *H. pylori* mutants that show a reduced ability to infect mice (Ottemann & Lowenthal, 2002).

In order to elucidate the molecular mechanism by which MotB molecules associate within the stator unit and attach themselves to peptidoglycan, crystallographic studies have been initiated on this protein. The crystallization of a 132-residue C-terminal fragment of *H. pylori* MotB has recently been reported (Roujeinikova, 2008). In this paper, the cloning, overexpression, purification, crystallization and preliminary X-ray diffraction analysis of the full-length protein are described.

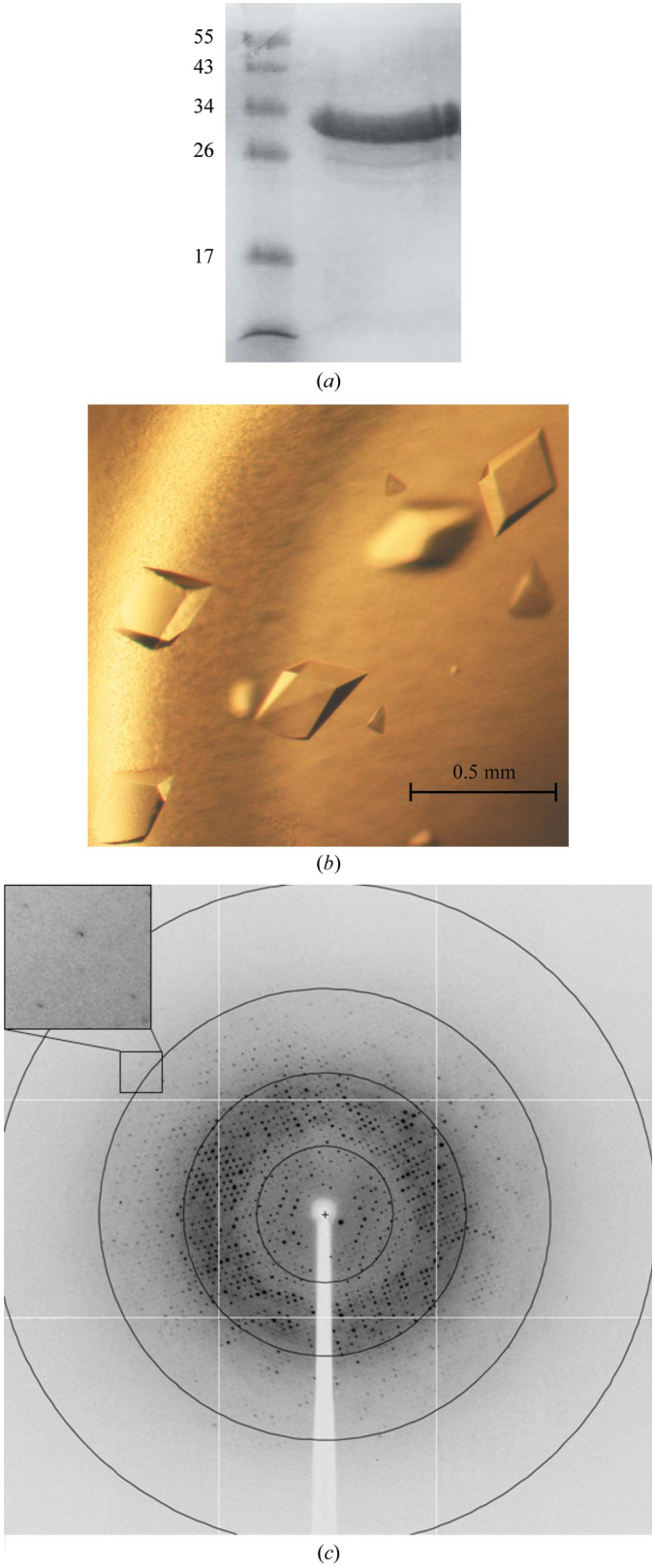

Figure 1
(*a*) SDS–PAGE (12%) analysis of purified recombinant *H. pylori* MotB (lane 2). Lane 1, PageRuler protein ladder (Fermentas; labelled in kDa). (*b*) Crystals of *H. pylori* MotB. (*c*) A representative 0.5° oscillation image of data collected from a MotB crystal using an ADSC Quantum 315r CCD detector on station ID14-4, ESRF, France. The magnified rectangle shows diffraction spots at a resolution of 2.0 Å. The resolution rings lie at 6.2, 3.1, 2.1 and 1.6 Å.

2. Materials and methods

2.1. Cloning and overexpression

The gene encoding *H. pylori* MotB (256 residues) was PCR-amplified from genomic DNA of *H. pylori* strain 26695 using the HotStar HiFidelity Polymerase kit (Qiagen) and primers CACCG-CTAAGAAAAACAAACCCACCGAATG (forward) and TCATT-CTTGCTGTTTGTGGGGATTG (reverse). The amplified fragment was cloned into the pET151/D-TOPO vector using the TOPO cloning kit (Invitrogen) to produce an expression vector featuring an N-terminal His_6 tag followed by the linker GKPIPNPLLGLDST-ENLYFQGIDPFT. The expression clone was confirmed by DNA sequencing. The vector was then transformed into *Escherichia coli* strain BL21 (Novagen). Cells were grown in LB medium containing 100 mg l^{-1} ampicillin at 310 K until an OD_{600} of 0.6 was reached, at which point overexpression of MotB was induced by adding 1 m*M* IPTG and growth was continued for a further 3 h. The cells were then harvested by centrifugation at 6000*g* for 20 min at 277 K.

2.2. Purification

Cells were lysed by sonication in a buffer containing 50 m*M* sodium phosphate pH 7.4, 100 m*M* NaCl and 1 m*M* PMSF. Cell debris was removed by centrifugation at 10 000*g* for 20 min. The membrane fraction was isolated by centrifugation at 100 000*g* for 2 h at 277 K. Western blot analysis was carried out on the membrane and soluble fractions using a WesternBreeze Chemiluminescent Detection kit (Invitrogen) with an anti-His-tag antibody (Sigma). The protein was mainly found in the soluble fraction. NaCl and imidazole were added to the soluble fraction to final concentrations of 500 and 10 m*M*, respectively, after which the supernatant was loaded onto a 5 ml Hi-Trap Chelating HP column (GE Healthcare) pre-washed with buffer *A* (20 m*M* sodium phosphate pH 7.4, 500 m*M* NaCl, 10 m*M* imidazole, 1 m*M* PMSF). The column was washed with 20 column volumes of buffer *B* (20 m*M* sodium phosphate pH 7.4, 500 m*M* NaCl, 80 m*M* imidazole) and the protein was eluted with buffer *B* containing 500 m*M* imidazole. The peak fractions were pooled and concentrated to 0.5 ml in a Vivaspin 10 000 Da molecular-weight cutoff concentrator and loaded onto a Superdex 75 HiLoad 26/60 gel-filtration column (GE Healthcare) equilibrated with 50 m*M* Tris–HCl pH 8.0, 200 m*M* NaCl. Analysis of the gel-filtration trace (not shown) suggested that MotB is mostly dimeric, with a tendency to form higher oligomers. The fractions containing MotB were identified using SDS–PAGE, pooled and dialysed overnight against 50 m*M* Tris–HCl pH 8.0. The purity of MotB was estimated to be greater than 95% (Fig. 1*a*). The protein migrates on SDS–PAGE with an apparent molecular weight of 32 kDa, which is close to the value calculated from the amino-acid sequence (28.8 kDa native protein plus 2.7 kDa N-terminal tag peptide).

2.3. Crystallization and preliminary X-ray analysis

Prior to crystallization, the protein solution in 50 m*M* Tris–HCl pH 8.0 was concentrated to 16 mg ml^{-1} (based on the Bradford assay; Bradford, 1976) and centrifuged for 20 min at 13 000*g* to clarify the solution. Initial screening of crystallization conditions was carried out by the sitting-drop vapour-diffusion method using an automated Phoenix crystallization robot (Art Robbins Instruments) and Crystal Screen, Crystal Screen 2 and PEG/Ion Screen (Hampton Research). The initial crystallization droplets contained 100 nl protein solution mixed with 100 nl reservoir solution and were equilibrated against 100 µl reservoir solution in a 96-well Intelliplate (Art Robbins Instruments). Crystals appeared after three weeks from condition No.

Table 1
Data-collection statistics.

Values in parentheses are for the highest resolution shell.

Wavelength (Å)	1.0
Resolution range (Å)	20–1.8 (1.9–1.8)
Completeness (%)	91 (91)
Observed reflections	162389
Unique reflections	30716
Mean $I/\sigma(I)$	16.8 (3.5)
$R_{\rm merge}$†	0.062 (0.331)

† $R_{\rm merge} = \sum_{hkl}\sum_i |I_i(hkl) - \langle I(hkl)\rangle| / \sum_{hkl}\sum_i I_i(hkl)$, where $I_i(hkl)$ is the intensity of the ith observation of reflection hkl.

23 of Crystal Screen 2, which contained 1.6 *M* ammonium sulfate, 100 m*M* MES monohydrate pH 6.5 and 10%(*v*/*v*) 1,4-dioxane. Refinement of this condition yielded the optimized composition of the reservoir solution, consisting of 2.1 *M* ammonium sulfate, 100 m*M* MES monohydrate pH 6.5 and 2.5%(*v*/*v*) 1,4-dioxane. Crystals (Fig. 1*b*) of maximum dimensions 0.3 × 0.3 × 0.4 mm were obtained using drops containing 3 µl protein solution mixed with 3 µl reservoir solution and equilibrated against 500 µl reservoir solution at 293 K. For data collection, crystals were flash-cooled to 100 K after soaking in a cryoprotectant solution consisting of the reservoir solution supplemented with 25%(*v*/*v*) glycerol. An X-ray data set was collected from the cryocooled native crystal to 1.8 Å resolution (Fig. 1*c*) on ESRF beamline ID14-4 (Grenoble, France). A total of 360 images were collected using a 0.5° oscillation width. All data were processed and scaled using the programs *MOSFLM* (Leslie, 1992) and *SCALA* (Collaborative Computational Project, Number 4, 1994). The statistics of data collection are summarized in Table 1.

3. Results and discussion

Autoindexing of the diffraction data using *MOSFLM* is consistent with a primitive tetragonal crystal system, class 422, with unit-cell parameters a = 75.2, b = 75.2, c = 124.7 Å. The diffraction patterns were examined using the program *HKLVIEW* (Collaborative Computational Project, Number 4, 1994). Systematic absences were observed along the a^* and c^* axes, with only reflections with $h = 2n$ and $l = 4n$, respectively, appearing to be present, which suggested that the crystals belong to one of the enantiomorphic space groups $P4_12_12$ or $P4_32_12$. Calculations of the Matthews coefficient (Matthews, 1977) suggested that the asymmetric unit is very likely to contain one molecule, with a $V_{\rm M}$ value of 3.4 Å^3 Da^{-1}.

In a search for a suitable model for the molecular-replacement approach, a *BLAST* sequence-similarity search against the structures deposited in the Protein Data Bank was carried out. One molecule with a moderate degree of homology to the C-terminal part of MotB has been identified. The 109-residue periplasmic domain of peptidoglycan-associated lipoprotein (PAL) from *E. coli* (PDB code 2aiz; Parsons *et al.*, 2006) and the putative peptidoglycan-binding domain of MotB (residues 125–256) share 26% sequence identity in a 102-residue overlap. However, the search model based on the PAL fragment would only constitute 43% of the full-length MotB structure. Given the limited level of sequence identity, the molecular-replacement approach with this model was not used. Our efforts are currently being directed towards identifying heavy-atom derivatives and the solution of the structure using the multiwavelength anomalous dispersion or multiple isomorphous replacement methods.

The genomic DNA of *H. pylori* strain 26695 was a gift from Dr Nicola High (University of Manchester). We thank Hassan Belrhali at the European Synchrotron Radiation Facility (Grenoble, France) and Patrick Bryant at the X-ray Crystallography Facility (University of Manchester) for assistance with data collection. This work was supported by a Wellcome Trust Research Career Development Fellowship to AR.

References

Blair, D. F. (2003). *FEBS Lett.* **545**, 86–95.
Bradford, M. M. (1976). *Anal. Biochem.* **72**, 248–254.
Chun, S. Y. & Parkinson, J. S. (1988). *Science*, **239**, 276–278.
Collaborative Computational Project, Number 4 (1994). *Acta Cryst.* D**50**, 760–763.
Covacci, A., Telford, J. L., Del Giudice, G., Parsonnet, J. & Rappuoli, R. (1999). *Science*, **284**, 1328–1333.
DeMot, R. & Vanderleydon, J. (1994). *Mol. Microbiol.* **12**, 333–334.
DeRosier, D. J. (1998). *Cell*, **93**, 17–20.
Eaton, K. A., Morgan, D. R. & Krakowska, S. (1992). *J. Med. Microbiol.* **37**, 123–127.
Hirota, N. & Imae, Y. (1983). *J. Biol. Chem.* **258**, 10577–10581.
Leslie, A. G. W. (1992). *Jnt CCP4/ESF–EACBM Newsl. Protein Crystallogr.* **26**.
Manson, M. D., Tedesco, P., Berg, H. C., Harold, F. M. & Van der Drift, C. (1977). *Proc. Natl Acad. Sci. USA*, **74**, 3060–3064.
Matthews, B. W. (1977). *The Proteins*, edited by H. Neurath & R. L. Hill, Vol. 3, pp. 468–477. New York: Academic Press.
Ottemann, K. M. & Lowenthal, A. C. (2002). *Infect. Immun.* **70**, 1984–1990.
Parsons, L. M., Lin, F. & Orban, J. (2006). *Biochemistry*, **45**, 2122–2128.
Roujeinikova, A. (2008). *Acta Cryst.* F**64**, 277–280.
Tomb, J. F. *et al.* (1997). *Nature (London)*, **338**, 539–547.
Uemura, N., Okamoto, S., Yamamoto, S., Matsumura, N., Yamaguchi, S., Yamakido, M., Taniyama, K., Sasaki, N. & Schlemper, R. J. (2001). *N. Engl. J. Med.* **345**, 784–789.
Yoshiyama, H. & Nakazawa, T. (2000). *Microbes Infect.* **2**, 55–60.
Zhou, J., Sharp, L. L., Tang, H. L., Lloyd, S. A., Billings, S., Braun, T. F. & Blair, D. F. (1998). *J. Bacteriol.* **180**, 2729–2735.